Utility of Quantitative Susceptibility Mapping in Neuroradiology: Initial Clinical Experience at a Tertiary Referral Hospital

Yangsean Choi, M.D., Ph.D.[1]; Sugil Kim, Ph.D.[2]

[1]Department of Radiology, Asan Medical Center, Seoul, Republic of Korea
[2]MR Research Collaboration, Siemens Healthineers Ltd, Seoul, Republic of Korea

Introduction

Quantitative susceptibility mapping (QSM) is an advanced imaging technique that provides quantitative information on tissue magnetic susceptibility derived from phase images. Since its introduction 10 years ago [1], QSM has been extensively researched as an imaging biomarker in neuroimaging to investigate various pathological processes, including iron deposition, hemorrhage, calcification, and myelin integrity [2]. However, the time-consuming manual processing required for QSM has been a significant barrier to its implementation in clinical practice. To facilitate the broader application of QSM, there is a pressing need for automated processing capabilities on magnetic resonance (MR) workstations.

A recent research package[1] from Siemens Healthineers as described in reference [3] has enabled inline QSM processing at the scanner. At Asan Medical Center in Seoul, South Korea, six MAGNETOM Vida scanners equipped with the QSM[1] research sequence are currently in operation. This has provided neuroradiologists with a unique opportunity to explore the wide spectrum of neurological diseases where QSM offers additional clinical insights. In this article, we discuss the clinical utility of QSM in neuroradiology, supported by various clinical case series.

MR acquisition parameters

The images presented in the clinical cases were acquired using a 3T MRI scanner (MAGNETOM Vida, Siemens Healthineers, Erlangen, Germany) with a 64-channel head/neck coil and 3D-GRE acquisition. Quantitative susceptibility maps were subsequently generated using the Total Generalized Variation (TGV) algorithm [4]. Detailed imaging parameters are summarized in Table 1.

Parameters	QSM
Field of view (mm)	256 × 176
Slice thickness (mm)	2.0
Slice per slab	68
Slice oversampling (%)	5.9
Spatial resolution (mm^3)	0.5 × 0.5 × 2.0
Matrix size	480 × 480
Partial Fourier (phase)	7/8
Orientation	Axial
TR (ms)	40.7
TE (ms)	5.4–36.8 (7 TE)
Flip angle (deg)	20
Bandwidth (Hz/pixel)	400
Acceleration mode	GRAPPA
Acceleration factor	2
QSM mode	TGV
Scan time (min:sec)	4:50

Table 1: Acquisition parameters for the QSM protocol.

[1]*Work in progress. The application is currently under development and is not for sale in the U.S. and in other countries. Its future availability cannot be ensured.*

Case 1

A 37-year-old man with highly active relapse-remitting multiple sclerosis (MS) presented to our neurology clinic with impaired fine motor functions. The patient had had eight recurrent attacks in the past two years and was being treated with Tecfidera (dimethyl fumarate).

In MS, chronic active lesions were previously identifiable only at autopsy. Before the advent of QSM, non-enhancing lesions with paramagnetic rims could be visualized using 7T MRI scanners; however, they can now be readily detected on QSM performed with 3T MRI scanners. These paramagnetic rims are indicative of ongoing inflammatory demyelination at the lesion periphery, remyelination failure, and axonal degeneration. Notably, chronic active lesions are associated with a more aggressive disease course, and can occur even in patients undergoing treatment with disease-modifying therapies [5]. Therefore, the long-term monitoring of chronic active lesions using QSM provides critical information regarding patient disability and the assessment of treatment response.

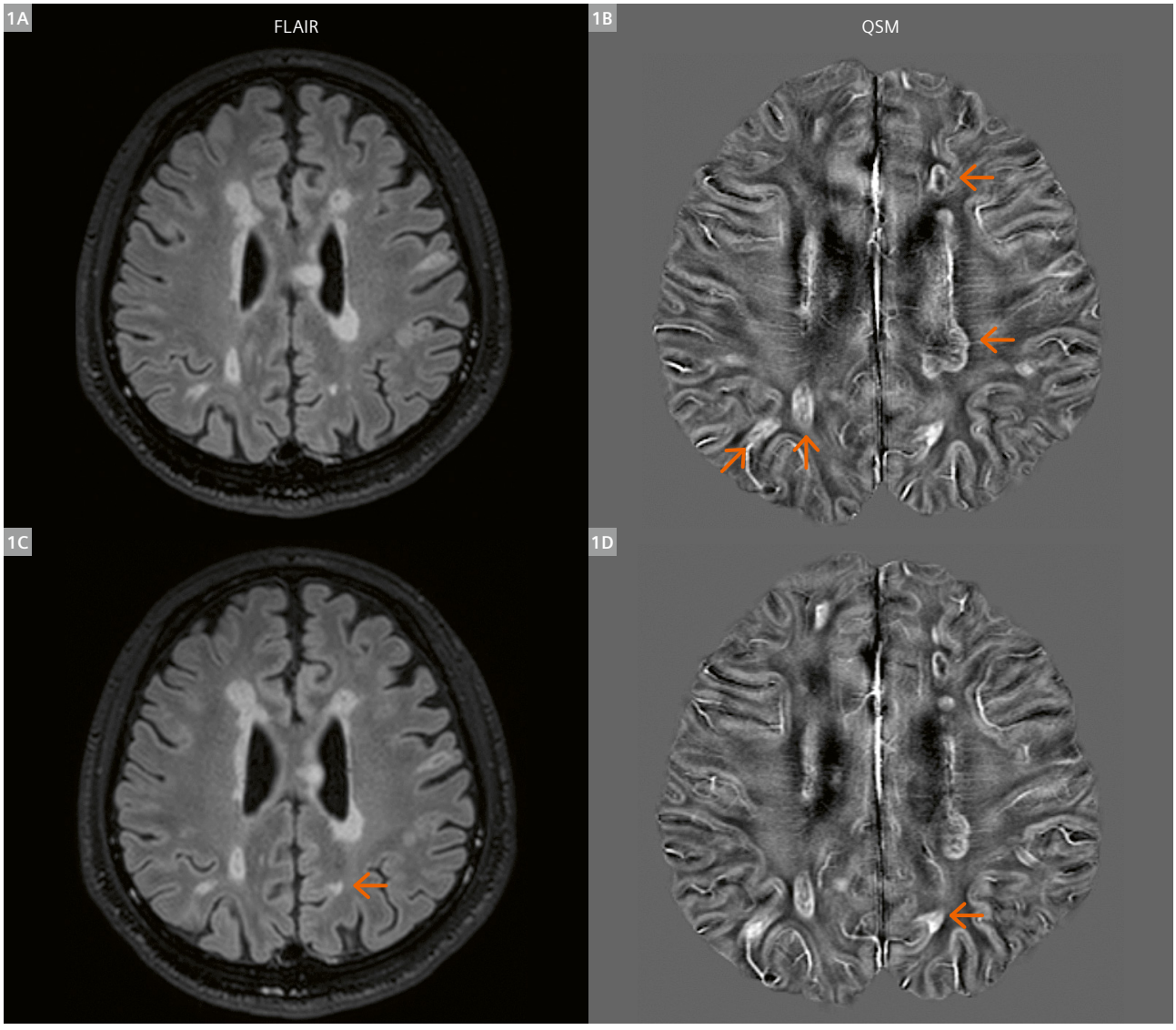

1 **FLAIR (left) and QSM (right) images of a 37-year-old man with highly active relapse-remitting MS.**
(Top) The FLAIR image **(1A)** shows multiple ovoid hyperintense lesions in the periventricular and deep white matter regions, without contrast enhancement (not shown). These could be considered chronic MS plaques. However, on QSM **(1B)**, these lesions display distinctive paramagnetic rims (red arrows), indicating that they are chronic active MS plaques.
(Bottom) The FLAIR image **(1C)** reveals a subcortical lesion with subtle hyperintensity in the left parietal lobe (red arrow), which is better visualized on QSM **(1D)** as a hyperintense paramagnetic lesion. QSM provides better delineation of the extent of paramagnetic MS plaques compared with FLAIR.

Case 2

A 77-year-old woman presented with progressive right-sided weakness and dysarthria that had begun one day prior. The patient had undergone spinal surgery two days earlier.

QSM can measure local venous oxygen saturation by detecting paramagnetic deoxyhemoglobin in venous vessels [6]. Increased magnetic susceptibility in cortical veins has been observed on QSM in the ischemic hemisphere of stroke patients. This finding is hypothesized to reflect an elevated deoxyhemoglobin content due to an increased oxygen extraction fraction [7, 8]. In cases where tissue perfusion is restored, prominent cortical veins with high susceptibility are expected to resolve, as observed in this case. Therefore, the qualitative evaluation of cortical veins on QSM could serve as a valuable imaging marker for assessing treatment response in patients with ischemic stroke.

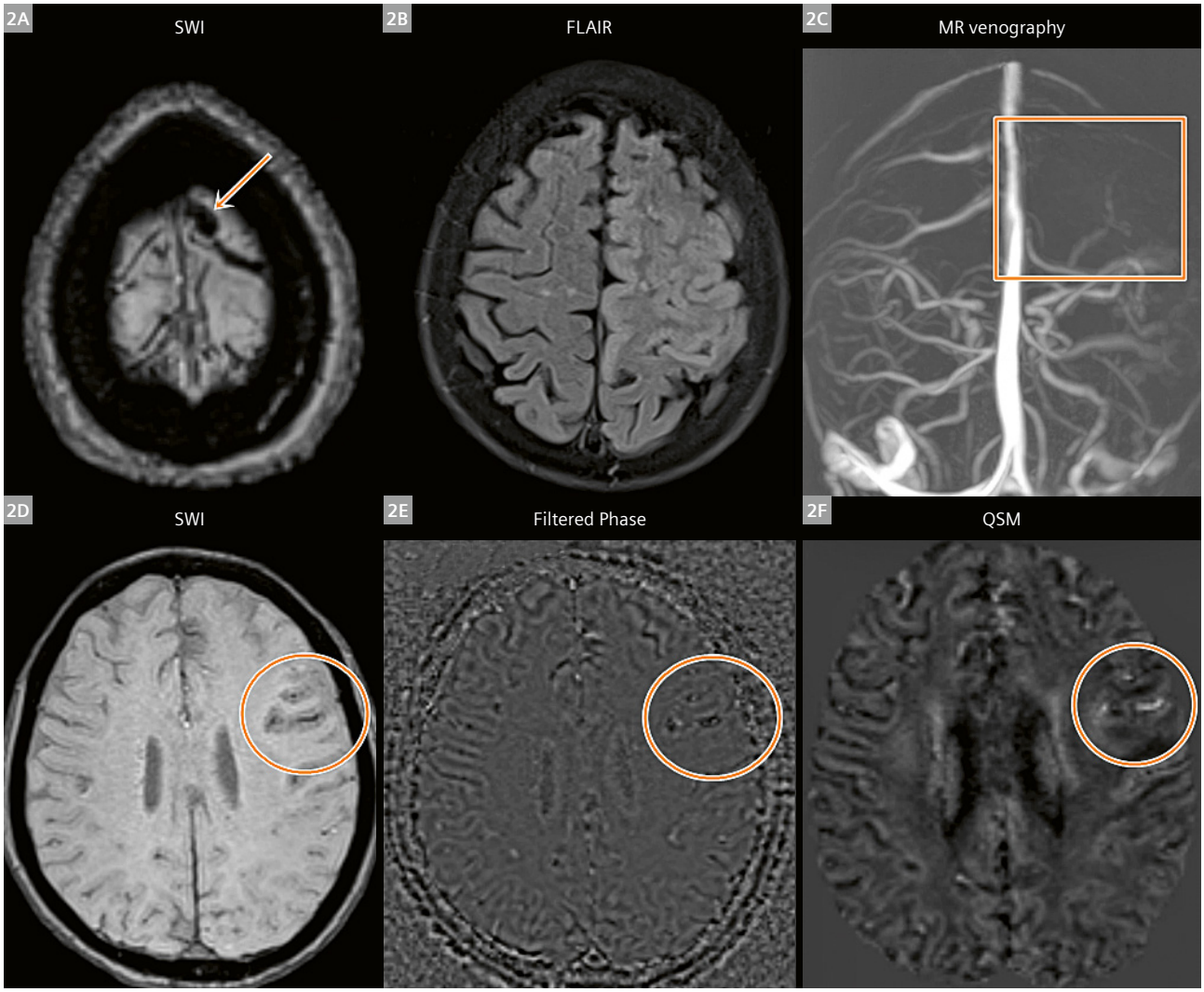

2 (Top) SWI **(2A)** shows a nodular dark signal intensity in the left upper cortical vein, suggesting a venous thrombus (arrow). The FLAIR image **(2B)** demonstrates diffuse gyral edema and hyperintensity in the left frontoparietal lobe. MR venography **(2C)** reveals a signal loss in the left vein of Trolard and left cortical veins (square).
(Bottom) On SWI **(2D)**, curvilinear dark signal intensities are visible in the left frontal sulci (circle). On the filtered phase image **(2E)**, these corresponding curvilinear dark signal intensities remain dark (circle), indicating that they may not be paramagnetic. However, on QSM **(2F)**, the corresponding areas show bright paramagnetic susceptibilities (circle), confirming the presence of deoxygenated cortical veins due to venous stasis.

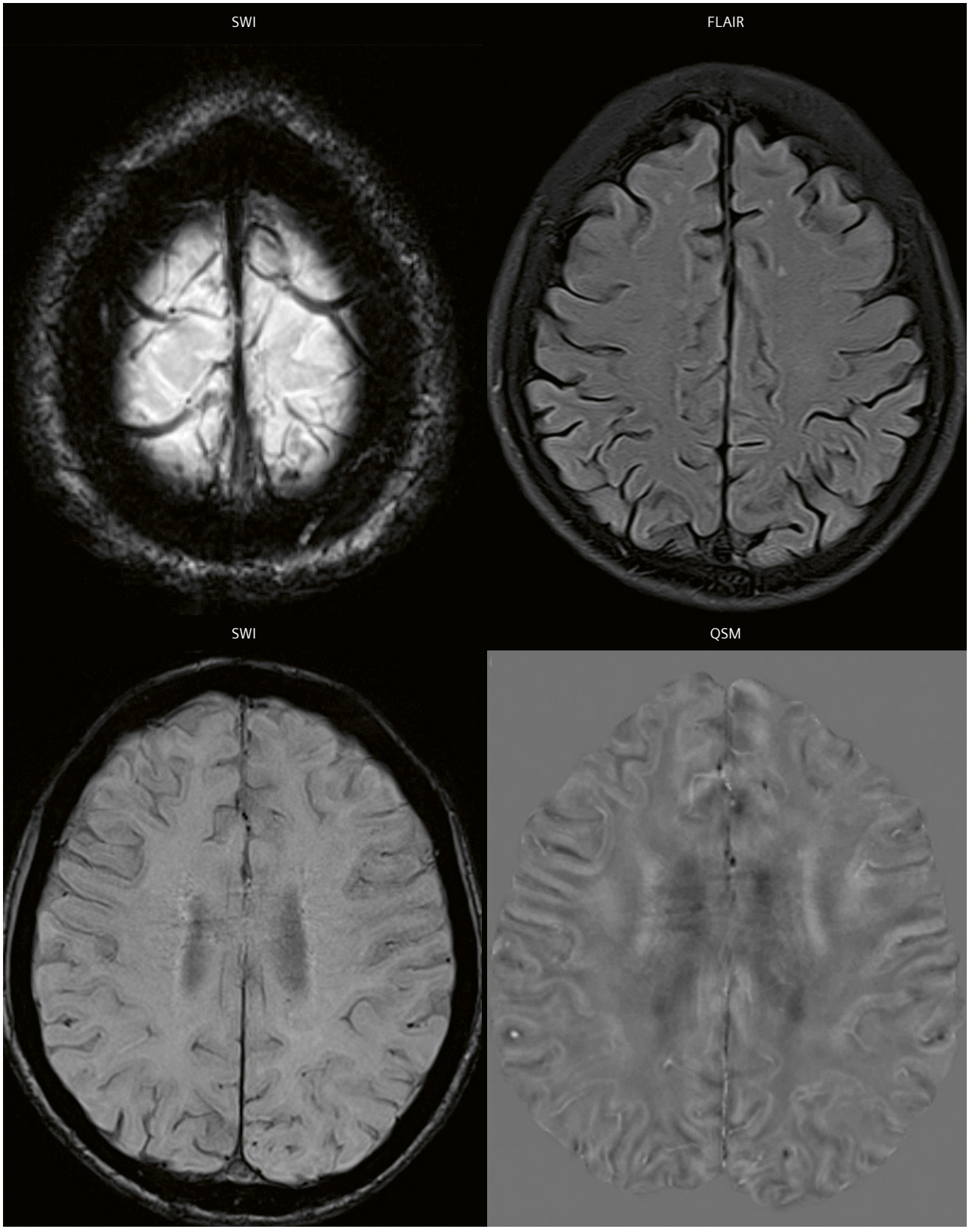

3 The patient was treated with anticoagulation. On imaging at one-month follow-up, the venous thrombus, gyral FLAIR hyperintensities, and deoxygenated cortical veins had all resolved.

Case 3

A 59-year-old man underwent a brain CT scan due to dizziness and was referred to our center for further evaluation of a nodular hyperdense lesion in the left occipital lobe.

QSM can differentiate between microhemorrhages and microcalcifications by detecting their opposite phase shifts, thereby aiding in the differential diagnosis. Conventional MRI sequences, such as T2*-weighted imaging and SWI, cannot provide this information since both show nonspecific low signal intensities for calcifications and hemorrhages. While CT imaging can often differentiate Conventional between calcifications and hemorrhages based on differences in attenuation, it can be challenging to reach a diagnosis when a small lesion presents with faint hyperdensity, as seen in this case. This case demonstrates how QSM can distinguish subtle differences in magnetic susceptibilities, offering a more precise characterization of such lesions.

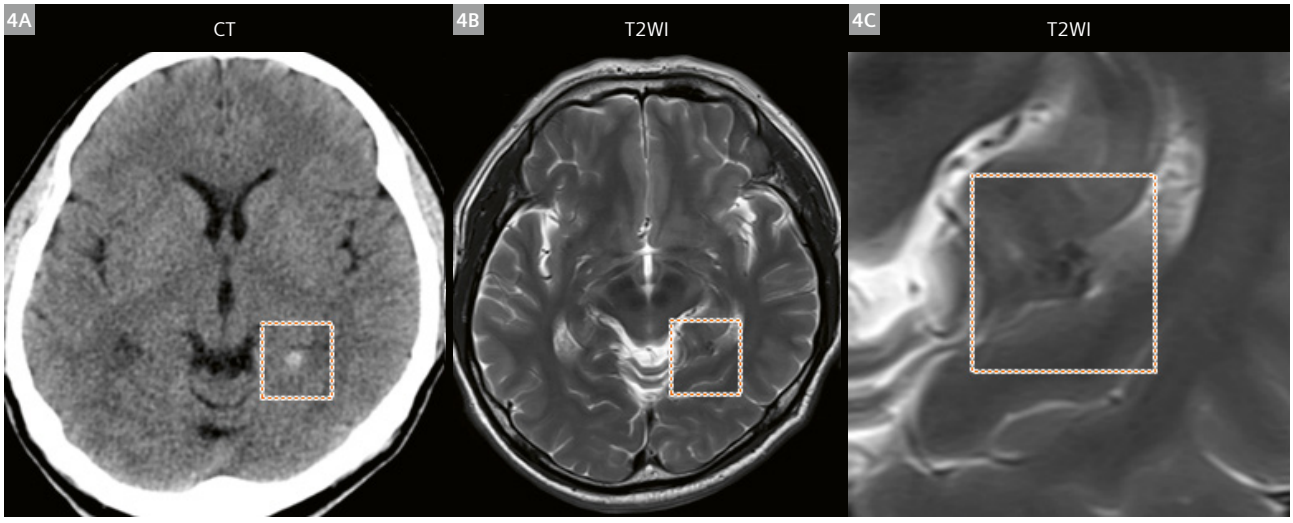

4 Brain CT scan **(4A)** shows a nodular hyperdense lesion in the left parietal cortical and left medial occipital lobe (square). On T2-weighted imaging (T2WI, **4B**), the lesion appears as a dark signal intensity (magnified view, **4C**). Based on these findings, the lesion would likely be diagnosed as a cavernous malformation.

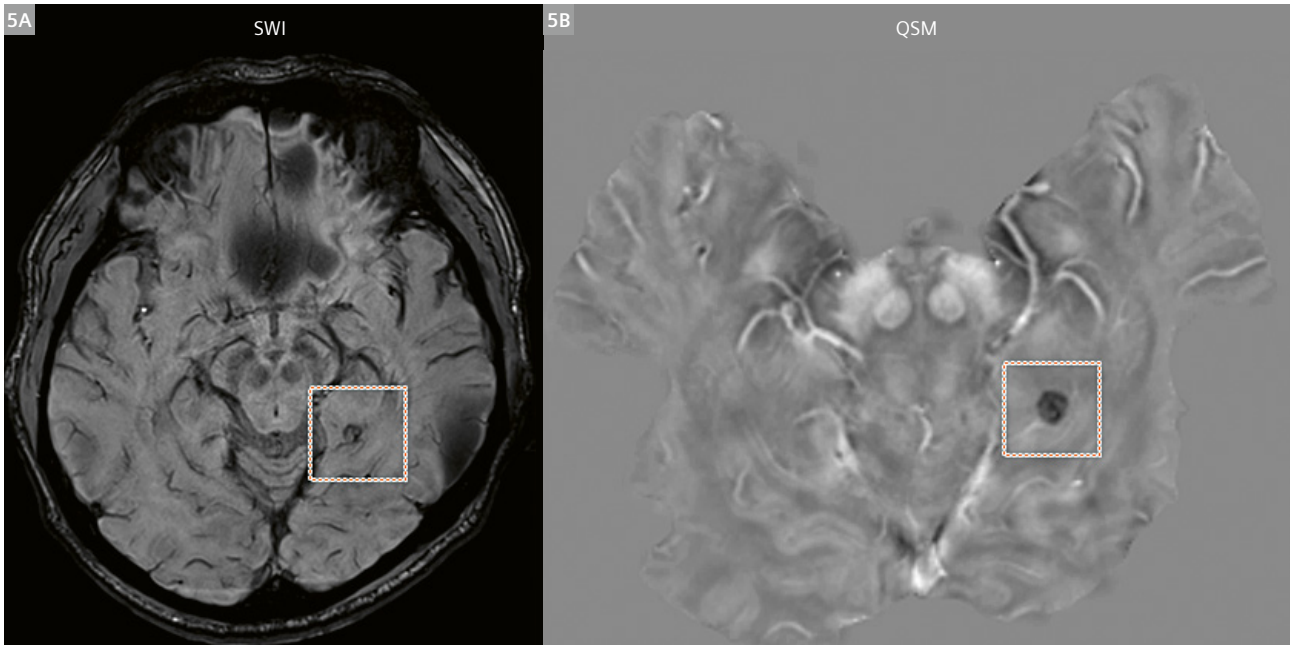

5 On both SWI **(5A)** and QSM **(5B)**, the lesion presents as a dark signal intensity, in contrast to the nearby venous structures which appear bright on QSM. This finding indicates that the lesion is a diamagnetic calcified granuloma, ruling out the possibility of cavernous malformation.

Case 4

An 81-year-old woman presented to the neurosurgery outpatient clinic for an incidentally discovered mass in the fourth ventricle on brain MRI.

This case demonstrates the clinical utility of QSM in differentiating microcalcification from microbleeds. Typically, the differentiation occurs within the brain parenchyma, and its clinical significance is often limited to identifying cerebral microbleeds and cavernous malformations. In approximately 25% of cases, intratumoral speckled calcifications are present within the choroid plexus papillomas [9]. Therefore, in brain tumor cases where imaging features such as speckled microcalcifications provide an important clue for accurate diagnosis, QSM can be highly beneficial for radiologists.

Conclusion

Quantitative Susceptibility Mapping (QSM) is an advanced imaging technique that quantifies tissue magnetic susceptibility, aiding in the assessment of neurological conditions like iron deposition, hemorrhage, and myelin integrity. While the clinical adoption of QSM has been limited by the need for manual processing, recent advancements, such as automated QSM processing on MAGNETOM Vida scanners, have made it more accessible for routine clinical use.

This paper highlights the clinical utility of QSM using case studies that show the following: detecting chronic active lesions in multiple sclerosis, assessing venous stasis in stroke, distinguishing between microbleeds and microcalcifications, and identifying microcalcifications in brain tumors. These examples demonstrate the robust ability of QSM to provide precise diagnostic information, making it a valuable tool that complements traditional imaging techniques and enhances diagnostic accuracy in neuroradiology. As technology continues to evolve, QSM is poised to become an integral part of neuroradiological practice.

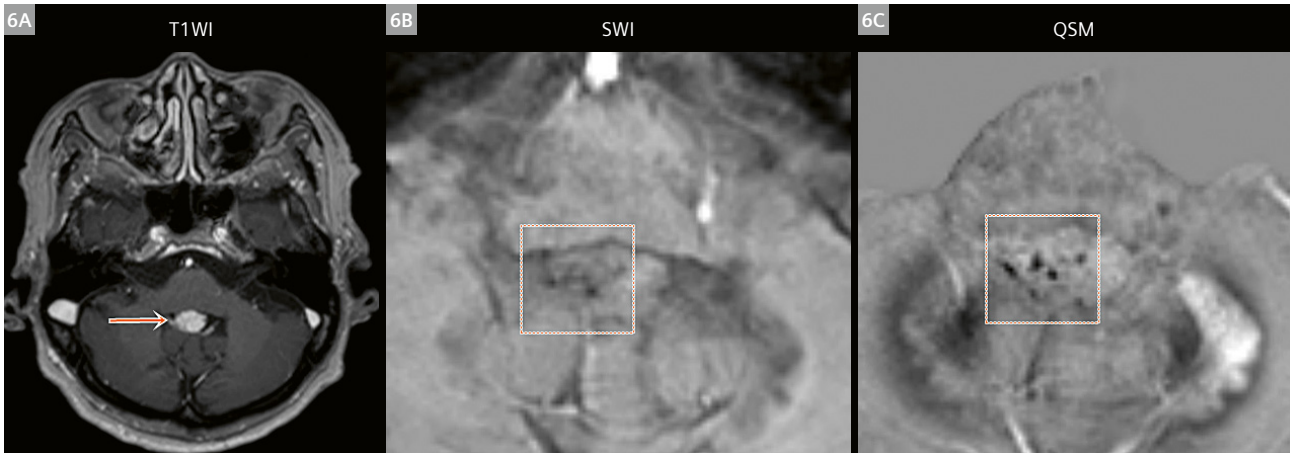

6 A 3D contrast-enhanced T1-weighted image **(6A)** shows a circumscribed solid enhancing mass within the fourth ventricle (arrow). On SWI **(6B)**, there are several indistinct foci of dark signal intensities (square). On QSM **(6C)**, the corresponding area displays clear foci of dark signal intensity, indicating the presence of microcalcifications.

Acknowledgments

The authors thank Dr. Josef Pfeuffer, Application Development, Siemens Healthineers, Erlangen, Germany, for providing the QSM research package for this study.

Contact

Assistant Professor Yangsean Choi, M.D., Ph.D.
Department of Radiology
Asan Medical Center
88 Olympic-ro 43-gil, Songpa District
Seoul
Republic of Korea
Tel.: +82 1688-7575
email.please@amc.seoul.kr

Sugil Kim, Ph.D.
MR Research Collaboration
Siemens Healthineers Ltd
SHS APJ KOR DI RC
14, Seocho-daero 74-gil
Seoul Teukbyeolsi 06620
Republic of Korea
sugil.kim@siemens-healthineers.com

References

1 Haacke EM, Liu S, Buch S, Zheng W, Wu D, Ye Y. Quantitative susceptibility mapping: current status and future directions. Magn Reson Imaging. 2015;33(1):1–25.
2 Fushimi Y, Nakajima S, Sakata A, Okuchi S, Otani S, Nakamoto Y. Value of Quantitative Susceptibility Mapping in Clinical Neuroradiology. J Magn Reson Imaging. 2024;59(6):1914–1929.
3 Pfeuffer J, Eckstein K, Stewart AW, Nickel D, Jin J, Meyer H, et al. Advances in Susceptibility-Weighted Imaging (SWI) and Quantitative Susceptibility Mapping (QSM). ↗ MAGNETOM Flash. 2024;87(2):88–98.
4 Stewart AW, Robinson SD, O'Brien K, Jin J, Widhalm G, Hangel G, et al. QSMxT: Robust masking and artifact reduction for quantitative susceptibility mapping. Magn Reson Med. 2022;87(3):1289–1300.
5 Absinta M, Sati P, Masuzzo F, Nair G, Sethi V, Kolb H, et al. Association of Chronic Active Multiple Sclerosis Lesions With Disability In Vivo. JAMA Neurol. 2019;76(12):1474–1483.
6 Haacke EM, Tang J, Neelavalli J, Cheng YC. Susceptibility mapping as a means to visualize veins and quantify oxygen saturation. J Magn Reson Imaging. 2010;32(3):663–76.
7 Ward PGD, Fan AP, Raniga P, Barnes DG, Dowe DL, Ng ACL, et al. Improved Quantification of Cerebral Vein Oxygenation Using Partial Volume Correction. Front Neurosci. 2017;11:89.
8 Probst J, Rohner M, Zahn M, Piccirelli M, Pangalu A, Luft A, et al. Quantitative susceptibility mapping in ischemic stroke patients after successful recanalization. Sci Rep. 2021;11(1):16038.
9 Yan C, Xu Y, Feng J, Sun C, Zhang G, Shi J, et al. Choroid plexus tumours: classification, MR imaging findings and pathological correlation. J Med Imaging Radiat Oncol. 2013;57(2):176–83.